Proceedings World Geothermal Congress 2020+1
Reykjavik, Iceland, April - October 2021

Fracture Permeability in a Pervasively Fractured Rock Mass: the Role of Regional Tectonics at Te Mihi, Wairakei Geothermal Field, New Zealand

Cécile MASSIOT[1], David D. MCNAMARA[2], Sarah D. MILICICH[1], Pilar VILLAMOR[1], Katie MCLEAN[3], Fabian SEPULVEDA[3], Will F. RIES[4]

[1]GNS Science, 1 Fairway Drive, Avalon, Lower Hutt, 5010, New Zealand

[2]Department of Earth, Ocean and Ecological Sciences, University of Liverpool, UK

[3]Contact Energy Ltd, Wairakei Power Station, Taupo, New Zealand

[4]Institut für Geographie und Regionalforschung, University of Vienna

c.massiot@gns.cri.nz

Keywords: Structural permeability, Wairakei Geothermal Field, downhole measurement, borehole images, LiDAR, regional tectonics, GPSS

ABSTRACT

Surface and downhole fracture mapping in the Taupō Volcanic Zone (TVZ), New Zealand, highlights that, although fractures and faults occur pervasively, only a portion of these structures supply geothermal fluids. Detailed fault mapping and borehole image logs were acquired prior to commissioning the Te Mihi power station in the Wairakei Geothermal Field to 1) identify areas of active-fault-related seismic hazard; 2) assist with site selection for the power station (commissioned in 2014); and 3) reservoir characterisation. This work also improved our understanding of structural trends and associated permeability of the field and the wider region.

The four borehole image logs show pervasive fracturing with orientations and maximum horizontal stress orientations (S_{Hmax}) consistent with the regional rifting, and fractures well-oriented for slip in a normal stress regime. Fractures are mainly steeply dipping (more than 70°) with dominant NE-SW strike, and secondary E-W and N-S strike. S_{Hmax} is NE-SW to NNE-SSW, with small-scale rotations related to potential recently active fractures and nearby faults. Based on correlation with completion test data, we observe that only a portion of the structures imaged with downhole tools supply geothermal fluids. Fractures in permeable zones are typically 1) of low amplitude and seen on the travel-time image of acoustic images; and 2) of low-resistivity fractures with high-resistivity haloes on resistivity images, although similar fracture characteristics are also observed outside permeable zones. In addition, permeable zones preferentially contain high fracture density and wide aperture fractures.

Tectonic structure changes substantially along rift strike (NE-SW) in the Te Mihi area, with the deformation of the NW-dipping, 045° striking Kaiapo and Whakaipo faults becoming more spatially distributed. Detailed surface mapping at Te Mihi using LiDAR reveals that Te Mihi is located at an intersection between two normal dip-slip fault sets: one striking 045° and another 060-070°. 3D fault models defined from local well stratigraphy also show fault terminations, splays and intersections, with permeable zones non-systematically coinciding with individual strands of the Kaiapo Fault. Regional plate motions, indicated by Global Navigation Satellite System (GNSS) velocity vectors in the Taupō Rift-Forearc region, show a clear change from a SE direction within the Taupō Rift to an SSE direction within the forearc. We propose that this change of direction allows the two normal fault orientations mapped on surface to be active simultaneously within the Taupō Rift, although the SE extension is dominantly reflected in the present-day S_{Hmax} direction in the boreholes. This biaxial extension may enhance fault dilation, connectivity, and thus permeability, supporting upflow in the Te Mihi area with fluid pathways dominantly controlled by the fault strands and local fracture connectivity. We propose that regions in the Taupō Rift where NE-SW and ENE-WSW to E-W trends intersect are areas that have experienced bi-axial extension, with higher potential for permeability. Considering regional tectonics is thus useful in assessing large-scale controls on permeability.

1. INTRODUCTION

Fractures and faults are a key contributor to permeability in many geothermal fields (e.g., Braithwaite et al., 2002; Davatzes & Hickman, 2010; McNamara et al., 2015; Wilson & Rowland, 2016), but it remains difficult to characterise structures and their associated permeability for successful well targeting and reservoir monitoring (e.g., Hernandez et al., 2015). For example, only some areas of the Taupō Volcanic Zone (TVZ), New Zealand, with good potential for permeability, host an active geothermal field (Villamor et al., 2017a).

In an Andersonian normal faulting regime, like in the TVZ, fractures and faults striking parallel to the maximum horizontal stress (S_{Hmax}) direction and dipping 60° have in theory the highest tendency for slip and being permeable (Barton et al., 1995; Anderson, 1905). However, fractures observed in geothermal boreholes in the TVZ tend to have steeper (commonly ≥70°) dip magnitudes (McNamara et al., 2015; Massiot et al., 2013), and focal mechanisms previously documented in the Wairakei Geothermal Field, New Zealand, show normal to strike-slip mechanisms with similarly high dip magnitudes (Kim et al., 2014; Sepulveda et al., 2015). As S_{Hmax} directions have been observed to vary locally in geothermal boreholes of the TVZ (e.g., McNamara et al., 2015), it remains challenging to make prediction of fracture orientations with high slip tendency (e.g., Massiot et al., 2019). It is thus important to constrain in more detail the location and geometry of faults, and S_{Hmax} direction, for further targeting of critically stressed fractures with higher potential to be permeable.

Within the past decade, the acquisition of high-resolution digital elevation models (DEM) with LiDAR (Light Detection and Ranging) technologies, borehole image logs in geothermal wells, and development of 3D geological models, has open new opportunities for detailed structural studies in geothermal fields and surrounding regions, and implications for permeability. At the Te Mihi geothermal sector of the Wairakei Geothermal Field, detailed surface fault mapping has already allowed the Te Mihi Power Plant to be re-sited in an area outside the identified construction-avoidance envelope that conformed to the recommendations of the New Zealand Ministry for the Environment guidelines (Villamor et al., 2015).

Here we present key results from the detailed McNamara et al. (2019) multi-disciplinary structural study of the Te Mihi geothermal sector of the Wairakei Geothermal Field, in the wider regional tectonic context of the Taupō Rift and associated Hikurangi subduction zone (Figure 1). We present the new model where the oblique subduction of the Pacific Plate under the Taupō Volcanic Zone (TVZ) results in biaxial extension in the Taupō Rift, accommodated by NE-SW-striking normal faults in combination with E-W-striking normal faults. Based on the integrated analysis of permeability from well tests and fractures from image logs, we also discuss how to identify fractures that are most likely to be permeable, with guidelines generally applicable to other geothermal fields.

2. GEOLOGICAL SETTING

The Wairakei Geothermal Field is located within New Zealand's North Island, in the TVZ (Figure 1), the active, southern portion of the Lau-Havre-Taupō extensional back arc basin. The TVZ formed as a result of westward subduction of the Pacific Plate beneath the North Island (Begg & Mouslopoulou, 2010; Cole & Spinks, 2009; Wilson & Rowland, 2016).

Over the last 60 years more than 200 wells have been drilled in the Wairakei-Tauhara Geothermal System. The Te Mihi sector of the Wairakei Geothermal Field lies in the northwest part of the productive reservoir (Figure 1). The stratigraphy encountered by the boreholes used in this study comprises volcaniclastic rocks, rhyolites and ignimbrites (see the following for more detail: Bignall et al., 2010; Rosenberg et al., 2009; Rosenberg, 2017). Geological units are variably hydrothermally altered following a trend of increasing alteration rank and intensity with depth (Bignall et al., 2010).

The Wairakei Geothermal Field is underlain by a combination NE-SW to ENE-WSW striking faults and fault- controlled basins (Taupō-Reporoa basin to the NE and Te Mihi basin to the NW). It is also underlain by caldera related structures (Grindley, 1965; Wilson et al., 1984), and possible inferred NW-SE striking basement structure linked to the extension of Hauraki Rift structures to the north, which is inferred to offset the Taupō Rift axis there (Rowland and Sibson, 2001; Figure 1).

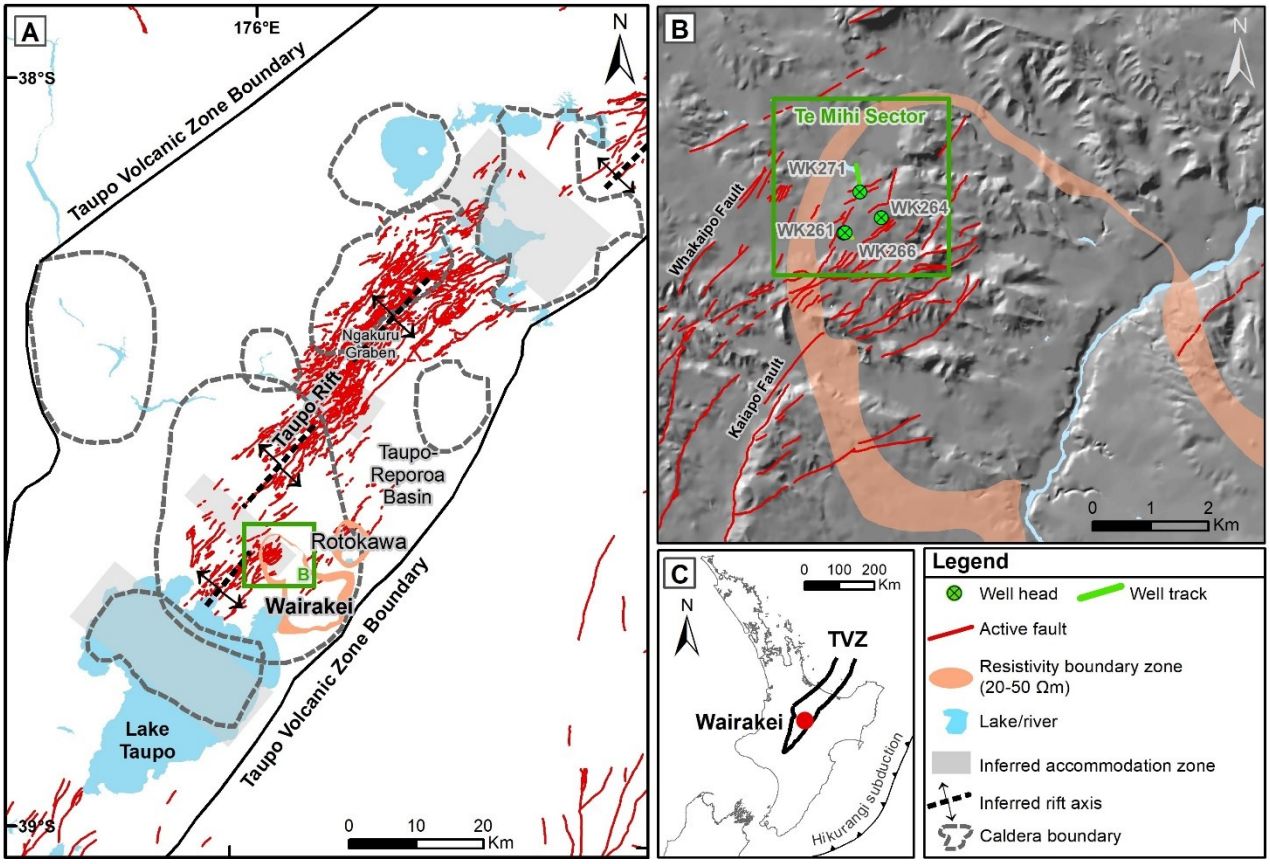

Figure 1: A) Map of the Taupō Volcanic Zone (TVZ) and its major structural elements. Active faults (Langridge et al., 2016), TVZ boundary (Wilson et al., 1995), inferred caldera boundaries (Wilson and Rowland, 2016), resistivity boundary zone, Rotokawa; (Risk, 2000), Wairakei; (Risk, 1984), inferred accommodation zones and rift axis (Rowland and Sibson, 2001). B) Map of the Te Mihi area of the Wairakei Geothermal Field showing structural elements, the locations of the four study wells. C) Map of the North Island of New Zealand showing the location of the TVZ and Wairakei.

3. DATA AND METHODS

This study combines structural data from surface active fault mapping; sub-surface fault mapping from 3D geological stratigraphic modeling (Rosenberg et al., 2009; Alcaraz, 2010); borehole image log interpretations of fractures and S_{Hmax} directions; and intervals of permeability interpreted from downhole measurements of pressure, temperature and fluid velocity (spinner; PTS).

Active faults are mapped on surface from their geomorphic expression, i.e., the identification of fault scarps that displace young landscape surfaces, in particular the extensive 25 ka Oruanui Ignimbrite constructional surface and younger valleys incised in that surface (Manville and Wilson, 2004). This study utilises a high-resolution DEM (pixels <1 m) derived from LiDAR data commissioned by the Waikato Regional Council (July 2009). The high resolution considerably improved fault scarp delineation compared to previous mapping that relied on modern (post-1990) and vintage (1940-1965) aerial photography, low-resolution DEMs (pixels 5-20 m), and field mapping (Villamor et al., 2015).

Borehole image logs, mapping the insides of the boreholes, have been acquired in four boreholes in the Te Mihi sector: three using the high-temperature acoustic borehole televiewer (BHTV) ABI85 (boreholes WK261, WK264, and WK266); and one using the resistivity Fullbore Formation Microimager (FMI; borehole WK271). Fractures interpreted from FMI logs are identified by contrasts in resistivity between the fracture and the adjacent borehole wall (Ekstrom et al., 1987; Davatzes and Hickman, 2010). Fractures in BHTV logs are revealed through their association with changes in borehole wall surface roughness or acoustic reflectivity (Zemaneck et al., 1970). Processing and interpretation of image logs following Massiot et al. (2015) and McNamara et al. (2019) yield the location; orientation; thickness at the borehole wall; and morphology of natural (fractures, faults, layers) and drilling-induced stress features. Lithological and textural interpretation of the resistivity image log is presented in Milicich et al. (2018, 2020).

Discrete permeable zones are identified from PTS logs, acquired under various injection rates. Results from PTS logs are correlated with image log structural interpretations to attempt to identify structural contributions to permeability (Davatzes & Hickman, 2010; Massiot et al., 2017; McLean & McNamara, 2011). The PTS interpretation method is described in detail in Massiot et al. (2017), and combines: 1) changes in temperature gradient during injection; 2) changes in temperature gradient during heatup; 3) steps in fluid velocity profiles from spinner data; 4) steps in the ratio of fluid velocity profiles from different injection rates; and 5) observation of the pressure control point during heatup. Permeable zones are classified as “major” when multiple indicators are clearly observed, thus indicate a higher contribution to fluid flow in the borehole, and “minor” otherwise. The robust interpretation of the location and extent of permeable zones is subsequently made by a joint interpretation of PTS and image log data, which improves the coarse resolution and uncertainty associated with interpretation of PTS data alone (Massiot et al., 2017).

4. RESULTS

4.1 Active Faults at Te Mihi

Active surface fault mapping shows that the Te Mihi sector of the Wairakei Geothermal Field is located at an intersection between two normal fault sets, one striking 045° and another striking 060-070°, with a few additional faults striking 030° (Figure 2). The 070° striking faults intersect many faults striking 045°.

Te Mihi is also located in a region where deformation is spatially distributed, with numerous fault traces of small scarp height. Indeed, ~10 km south of the field close to the Lake Taupō shore, there are 045°-striking faults with prominent fault scarps (120 m and 25 m high for the Kaiapo and Whakaipo faults, respectively) (Landridge et al., 2016, Leonard et al., 2010). A few kilometers north of Te Mihi, deformation becomes more focused and step eastwards to the Aratiatia Fault and northwestwards to the Orakonui Fault. The distributed faults of the Te Mihi area seem to tip out to the north of Te Mihi (Figure 2).

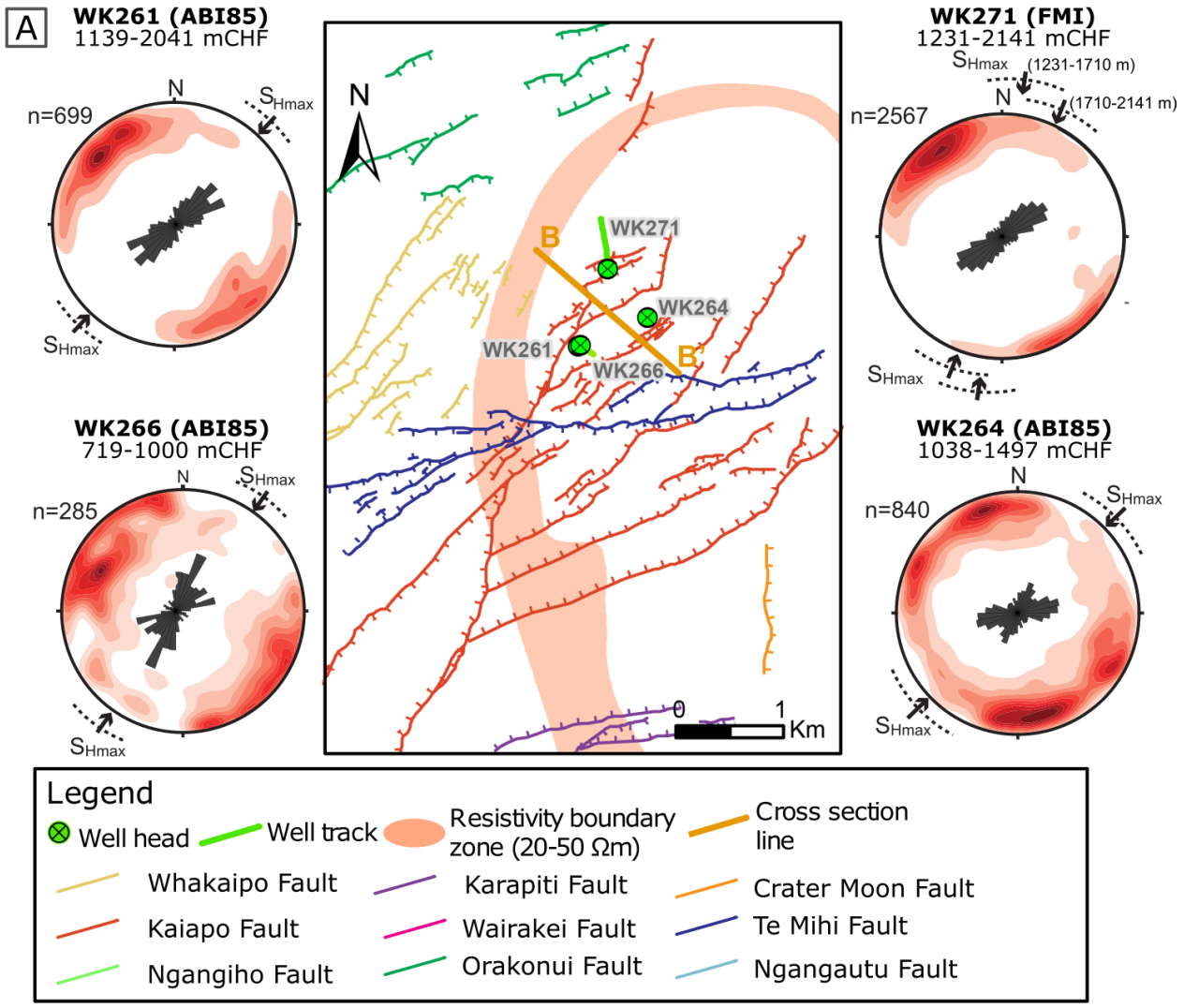

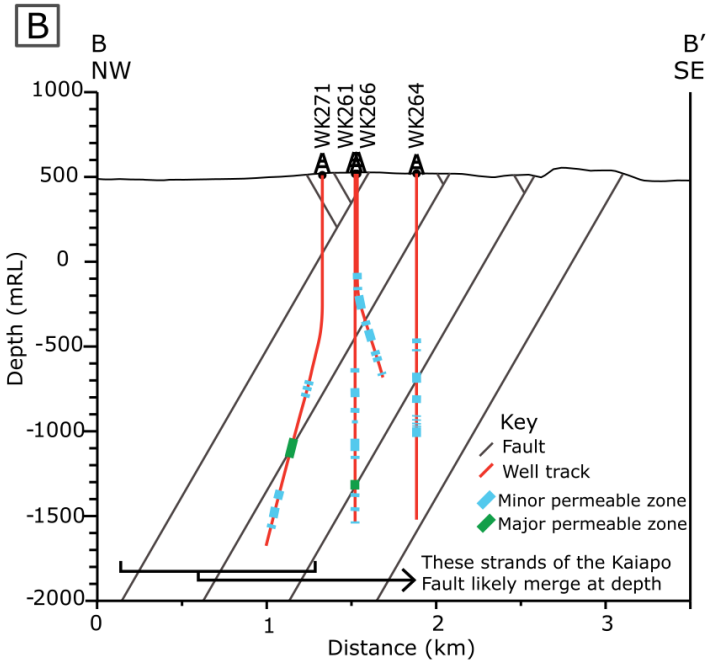

Figure 2: A) Interpreted structural map of the Te Mihi region. Regional fault strands are in the same colour. Ticks on faults denote the downthrown block (hanging wall). All stereonets are rose diagrams and Schmidt net, lower hemisphere, pole to planes, contoured using Fisher distributions for data corrected for orientation bias (Terzaghi, 1965; n = raw, uncorrected fracture count for each well; mCHF=metres below casing head flange). B) Cross-section (B-B', Figure 2A) showing where projected, mapped faults, dipping 70°, intersect well tracks of the four study wells.

4.2 Fracture and In-Situ Stress Orientations from Borehole Images

In the four study wells, the 4391 natural features observed are predominantly conductive fractures (80%; FMI log) or low acoustic amplitude fractures (~99%; BHTV logs). Few structures were classified as faults, i.e., showing a clear displacement or truncation of a feature over another. We note that reservoir-scale faults may not appear as features of "fault" morphology on the image log because of difference in scale. About 18% of the low acoustic amplitude fractures are seen on the travel time image and thus show an excavation at the borehole wall (Figure 3a). A small proportion (3%) of FMI natural features are halo fractures, appearing as low resistivity core and high resistivity halo (Figure 3b). Stress-induced features were drilling-induced tensile fractures (DITFs) and indicate the S_{Hmax} direction in this normal faulting stress regime, assuming that one stress component is vertical.

In the four studied boreholes, nearly 80% of fractures have dip magnitudes ≥70º, similar to other borehole image interpretations in the TVZ (Massiot et al., 2013; McNamara et al., 2015; Wallis et al., 2012). Fractures dominantly strike NE-SW to the SE (Figure 2). A subordinate fracture population striking E-W (dipping N and S equally) is observed in all wells except WK264 where the E-W striking fracture population dominates. An additional N-S striking subordinate fracture orientation is observed in well WK266, dipping both E and W. Dominant fracture strike and dip directions vary locally along each well and documented in detail in McNamara et al. (2019). Higher than average fracture density intervals were mostly located in partially-welded to welded-ignimbrites and rhyolite lava bodies (Milicich et al., 2020).

S_{Hmax} azimuth, defined from drilling-induced tensile fractures (DITFs), are NE-SW in wells WK261 and WK264; and NNE-SSW in wells WK271 and WK266 (Figure 2). Stress rotations that occur after the structure has slipped and disturbed the stress field, or because the structure is weak (e.g., filled with fault gouge; Fossen, 2016), are observed from borehole to field scale within these dominant orientations. Indeed, in WK271, S_{Hmax} changes from 018º-198º to 035º-215º at 1710 mCHF (meters below casing flange; equivalent to -1227 mRL, reference to sea level). This ~15° rotation of S_{Hmax} coincides with WK271 intersection with a projected fault plane on the 3D model. A large, active, NNE-SSW striking fault to the east of well WK271 may also explain the S_{Hmax} rotation. In addition, about half of the localised S_{Hmax} rotations at borehole scale occur over discrete fractures or clusters of fractures, identifying these as active structures (Figure 3c).

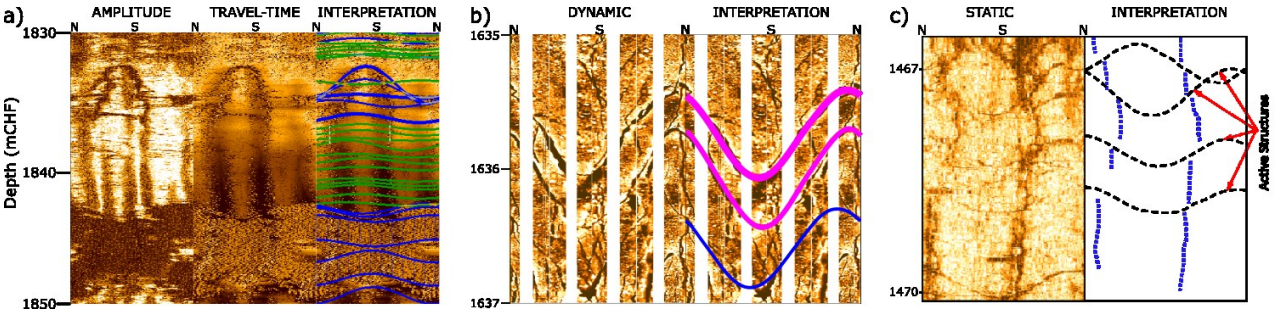

Figure 3: Characteristics of fractures predominantly observed in permeable zones. Note that fractures of these characteristics are also observed outside permeable zones (Massiot et al., 2017). a) Fractures of low acoustic amplitude seen on travel-time image (blue sinusoids; BHTV log). b) Conductive fractures with resistive halo (purple sunisoids; FMI log). c) Active structures (black sinusoids) with S_{Hmax} azimuth rotation (DITFs rotate; blue dotted lines).

4.3 Characteristics of potentially permeable fractures

Borehole image logs cannot indicate whether fractures are open or closed to fluid flow, which is why results from image log analysis need to be assessed in combination with PTS data to identify the characteristics of fractures in permeable zones, hence potentially permeable. PTS data used to identify permeable zones is at lower resolution than image logs, hence there are usually dozens of fractures in each permeable zones (Massiot et al., 2017). At Te Mihi, hosted in volcaniclastic and rhyolitic formations, several fracture characteristics are more common within rather than out of permeable zones:

(1) Fractures of low acoustic amplitude seen on travel-time image on BHTV logs

(2) Conductive fractures with high resistivity haloes on resistivity logs

(3) Active structures which are associated with local rotation of *in-situ* stress features (drilling-induced tensile fractures).

(4) Thicker-than-average fractures, noting that the thickness measured on image logs is the distance between two fracture or vein planes, rather than the hydraulic aperture which is the real empty space for fluids to go through. Fractures of the first two types are often thicker than average.

(5) Higher-than-average fracture density, caused by either faulting or lithological (mechanical) controls. At Te Mihi, lithologies with higher density include tuffs and welded ignimbrites in the Waiora and Tahorakuri formations, and massive and brecciated intervals within the rhyolite bodies

These characteristics help identifying *potential* permeable fractures in image logs, but fractures of these characteristics are also observed outside permeable zones. Low acoustic amplitude and conductive for acoustic and resistivity logs, respectively, can result from being open and filled with fluid (drilling or formation); or closed by minerals such as clay. In the four study boreholes, fracture orientation is similar within and out of permeable zones (with a few exceptions), so orientation information alone is not sufficient to identify which fractures are permeable. In pervasively fractured rocks like in the TVZ, these listed characteristics must be taken with caution and used in association with other datasets (cores, drill cuttings, other downhole measurements) to conclude that they are permeable.

4.4 Te Mihi: master and antithetic faults

Borehole images, surface fault mapping and 3D geological modelling show that faults in the Te Mihi area are steeply dipping (>70°), predominantly strike NE-SW and dip NW. In addition, there are numerous fault traces striking 030° and 060°, both of which have NW and SE dip directions (Figure 2a). Based on their large offsets, the NW-dipping faults are interpreted as master structures in the Te Mihi area (i.e., accommodate more deformation). These NW dipping faults splay from the main, NW dipping Kaiapo Fault trace to the south of the Te Mihi area, which cross-cuts the 060-090° striking fault traces within Te Mihi (Figure 2a-b).

In boreholes, fractures are dominantly dipping SE, opposite to the NW dipping master faults. We interpret these borehole fractures as representing antithetic substructures, resulting from (1) horse-tailing termination of the Kaiapo Fault; (2) intersection between the NE-SW striking Kaiapo Fault with E-W striking faults in the Te Mihi area; and (3) fault stepovers to the NE of Te Mihi. Faults are complex zones of tectonic deformation (Faulkner at al., 2010), and normal faults in an extensional setting, such as the Te Mihi region, can be associated with a variety of antithetic substructures occurring both along strike and at fault tips (horse-tailing), where major faults intersect, and at faults step-overs or bends (Faulds et al., 2011; Nicol et al., 1995; Peacock & Sanderson, 1991). Furthermore, an antithetic model is consistent with similar conclusions drawn from datasets elsewhere in the TVZ including borehole image fracture analysis in the nearby Rotokawa Geothermal Field (McNamara et al., 2015), fault mapping across the onshore TVZ (Begg & Mouslopoulou, 2010; Villamor et al., 2017b), and seismic profile interpretation in the offshore TVZ rift, the Whakatane Graben (Lamarche et al., 2006).

5. DISCUSSION

5.1 Regional tectonics and biaxial extension

Although the Taupō Rift is dominated by NE-SW-striking normal faults, there are also ENE-WSW to E-W-striking active faults (Villamor & Berryman, 2006). This 070°-090° strike is observed on surface mapping and borehole data at Te Mihi (this study) and in boreholes at the Tauhara Geothermal Field (SE of Te Mihi; Massiot and McNamara, 2013); along the southern margin of the Okataina Volcanic Centre (Villamor et al., 2017b); along sections of the 1987 ML 6.3 Edgecumbe normal fault surface rupture (Beanland et al., 1989); in the Ngakuru Graben (~30 km north of Wairakei; Figure 1), and inferred to continue to the west into the Ngakuru Graben axis (Downs et al., 2014); at the southern termination of the Taupō Rift (Villamor & Berryman, 2006); and as inherited basement faults outside the rift (Villamor et al., 2017b; Lee et al., 2011; Leonard et al., 2010). The presence of coeval active normal faults striking NE-SW and E-W suggests that extension is not uniaxial within these parts of the Taupō Rift given none of these fault sets show significant strike-slip components (Seebeck et al., 2014).

Re-injection and pressure regime history of the Wairakei-Tauhara Geothermal Field demonstrated that there are permeable connections in E-W and NW-SE directions (Milloy and Lim, 2012). These connections may be caused by matrix permeability in the brecciated top and within the Karapiti 2A Rhyolite at shallow depth (300-600 m; Milloy and Lim, 2012), but is also consistent with the potential presence of E-W-striking normal faults that we propose here, especially below 2000 m where it would be consistent with deep injection pressure change patterns.

We propose that, in the region between the North Island Dextral Fault Belt (NIDFB, Figure 5) and the Taupō Rift, and within regions of the Taupō Rift, the rotation of the forearc of the Hikurangi margin (Wallace et al., 2004; Figure 1) is partially accommodated by normal faulting on 070°- 090° striking faults. Villamor et al. (2017a) show preliminary mapping of 070°- 090° striking, active, and potentially active faults in this region that connect both the NIDFB and Taupō Rift fault belts (Figure 5). As 070°- 090° striking faults hit the eastern margin of the Taupō Rift, they interact and intersect with the dominant NE-SW striking faults there creating coexisting NW-SE and NNW-SSE directed extension (Figure 5b). Global Navigation Satellite System (GNSS) velocity vectors in the Taupō Rift-Forearc region show a clear change from a SE direction within the Taupō Rift to an SSE direction within the forearc (Beavan et al., 2016; Figure 4a). From the northern shore of Lake Taupō to the southern part of Okataina Volcanic Centre, the GNSS vector orientation change occurs abruptly at the eastern margin of the Taupō Rift. We suggest that along this section of the rift, the eastern margin is subjected to two extensional process: SE-directed rift extension caused mainly by slab roll back perpendicular to the slab contours (Seebeck et al., 2014, Williams et al., 2013); and a further opening by the forearc pull in an SSE direction (Wallace et al., 2004). We propose that the lateral component of the oblique plate conversion along the Hikurangi margin does not only produce rotation of the fore-arc block and strike-slip in the NIDFB (as suggested by Wallace et al., 2004), but also normal faulting in the eastern margin of the forearc block.

Two coeval pulling forces may also produce local changes in stress field orientations, with stress directions aligning themselves to whichever active structure is most proximal. However, our borehole data clearly shows a dominant stress field orientation with NW-SE directed extension with small scale variations. This suggests that: 1) the NW-SE extension is the dominant component of extension over the wider Te Mihi area and the NNW-SSW directed extension is only a smaller component; 2) the reorientation of stress from the E-W Te Mihi fault occurs over a small distance (<530 - 1080 m) or 3) that the N-S extensional component is temporal and occurs only intermittently.

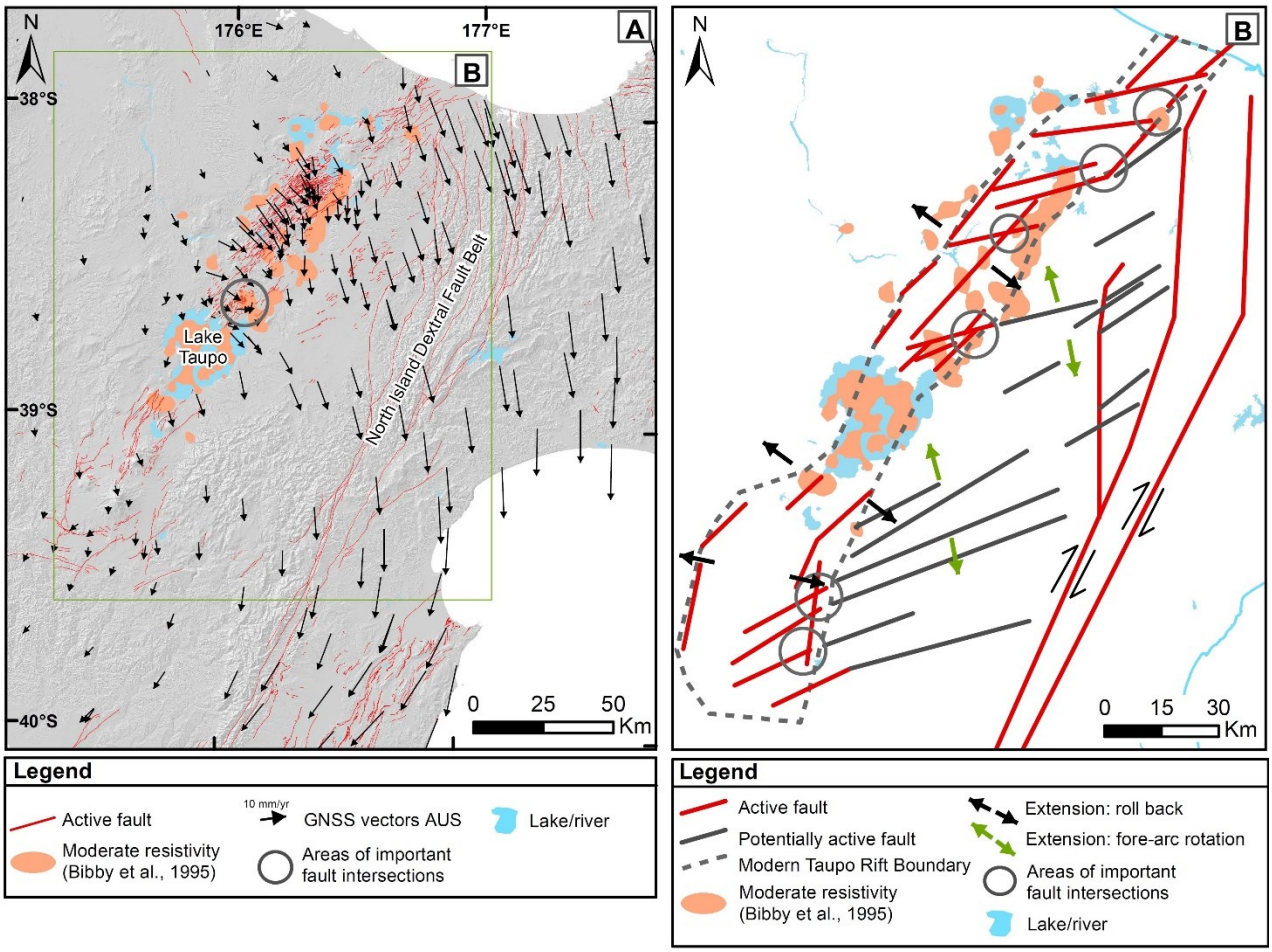

Figure 4: a) Map of faulting, GNSS vectors, and resistivity anomalies of the eastern North Island of New Zealand, b) Conceptual tectonic model of the TVZ highlighting spatial correlations of geothermal expression (resistivity anomalies) and potential zones of localised biaxial extension with intersecting, active, normal, NE-SW and E-W striking faults.

5.2 Regional controls on permeability in the TVZ

Regional tectonics affect the structural network configuration, and permeability potential (Barton et al., 1995; Townend et al., 2000; Jollie et al., 2015). Fractures which are optimally oriented for slip and dilation have a higher potential to be permeable. In theory, knowledge of the stress regime and fracture orientations should be sufficient for determining favourable fracture orientations and efficiently targeting permeable fractures. However, at Te Mihi, orientation alone is not a sufficient characteristic for identifying permeable zones, at field- or borehole-scales.

The Taupō Rift is pervasively fractured at several scales and depths, as demonstrated in this study. The regional tectonics of NW-SE extension result in a dominant NE-SW-striking structural fabric, with normal dip-slip motion. In an area like Te Mihi, where faulting is spatially distributed, it is useful to consider the larger tectonic settings to relate certain orientation to a possible faulting mechanism, and permeability potential. Indeed, while image logs provide detailed view of structures in boreholes, it is very rare to be able to determine the fault motions from image logs. Considering the regional tectonics of the Taupō Rift-Forearc region, we suggest that the 070°-090°-striking fractures at Te Mihi may reflect nearby normal faults which are active sporadically, with enhanced permeability.

At Te Mihi, some permeable zones, including two major ones, are located at the intersection between the borehole and a master fault as defined from surface mapping. This highlights that detailed surface mapping using LiDAR, potentially complemented by Ground Penetrating Radar and trenching (Villamor et al., 2015), can improve well targeting. Some of the permeable zones do not coincide with faults, which may relate to the smaller faults and fractures observed in image logs but with insufficient stratigraphic offset between wells and too small scarp at surface; or enhanced matrix permeability. On the other hand, permeable zones are not located everywhere in the pervasively fractured rock mass because of channelling occurring naturally even in fully connected fracture networks (Kissling and Massiot, 2020). At the TVZ scale, some areas favourable for structural permeability similarly to Te Mihi do not show evidence of an active hydrothermal system; these zones may consist of recharge zones (cold fluids going downwards), or lack sufficient connectivity to a heat source (Villamor et al., 2017a). Integrated, multi-scale structural and reservoir data interpretation, in the context of regional tectonics, is thus needed to unravel the characteristics and sources of permeability at reservoir and regional scales.

6. CONCLUSION

Mapping of fractures and faults from surface and sub-surface, at field- and borehole-scale in the Te Mihi sector of the Wairakei Geothermal Field show that this productive part of the field is characterised by distributed normal faults dominantly striking NE-SW, with likely master NW-dipping and antithetic SE-dipping faults. S_{Hmax} directions NE-SW is consistent with the Taupō Rift extending NW-SE, and the presence of multiple faults with recent slip of weak material such as gouge causing local rotations at 10s to 100s meters. Surface and downhole structure mapping also show a subordinate population of faults and fractures striking ENE-WSW to E-W. Based on data from other places in the TVZ, we infer that structures of this subordinate orientation also move in dip-slip mode (normal faults), and that this reflect a bi-axial extension of the Taupō Rift caused by the rotation of the forearc of the Hikurangi margin.

While the orientation of fracture in boreholes is not sufficient to identify which fractures are permeable, this study presents a series of characteristics for fractures having a higher permeability likelihood, based on correlation with PTS and drilling losses data. This are: (1) factures of low acoustic amplitude seen on travel-time image on BHTV logs; (2) conductive fractures with high resistivity haloes on resistivity logs; (3) active structures which are associated with local rotation of *in-situ* stress features; (4) thicker-than-average fractures; (5) zones with higher-than-average fracture density. These characteristics can serve as preliminary potential fracture permeability guideline, especially before finalising the localisation of permeable zones in boreholes. In addition, regional tectonics with the proposed bi-axial rift extension may explain some of the E-W flow pathways observed in the Wairakei Geothermal Field. Therefore, multi-scale structural analysis from borehole- to regional scale can help in identifying controls on permeability in geothermal fields.

ACKNOWLEDGEMENTS

The authors would like to acknowledge GNS Science and the New Zealand Ministry Business, Innovation and Employment for providing funding for this study through the New Zealand Geothermal Future research program. We also thank Contact Energy for the acquisition and contribution of the raw image log datasets utilised in the study, and for access to the 3D geological model of the reservoir. Thanks to the Waikato Regional Council for provision of LiDAR data used in this study. The authors also acknowledge support of this work by Haliburton Software and Services, a Haliburton Company through the use of Recall™ Borehole software.

REFERENCES

Alcaraz, S.A., Sépulveda, F., Lane, R., Rosenberg, M.D., Rae, A.J., and Bignall, G.: A 3-D Representation of the Wairakei Geothermal System (New Zealand) Using "Earth Research" Geothermal Visualisation and Modelling Software, *Transactions Geothermal Resources Council*, 34, (2010), 1020-1024.

Anderson, E. M.: The Dynamics of Faulting. Transactions of the Edinburgh Geological Society, 8(3), (1905). 387–402.

Barton, C.A., Zoback, M.D., and Moos, D.: Fluid Flow along Potentially Active Faults in Crystalline Rock, *Geology*, 23(8), (1995), 683-686, doi:10.1130/0091-7613(1995)023<0683:FFAPAF>2.3.CO;2.

Beanland, S., Berryman, K.R., and Blick, G.H.: Geological Investigations of the 1987 Edgecumbe Earthquake, New Zealand, *New Zealand Journal of Geology and Geophysics*, 32(1), (1989), 73-91.

Beavan, J., Wallace, L.M., Palmer, N., Denys, P., Ellis, S., Fournier, N., Hreinsdottir, S., Pearson, C., and Denham, M.: New Zealand GPS Velocity Field: 1995–2013, *New Zealand Journal of Geology and Geophysics*, 59(1), (2016), 5-14.

Begg, J.G., and Mouslopoulou, V.: Analysis of Late Holocene Faulting within an Active Rift using LIDAR, Taupo Rift, New Zealand, *Journal of Volcanology and Geothermal Research*, 190(1), (2010), 152–167, doi:10.1016/j.jvolgeores.2009.06.001.

Bignall, G., Rosenberg, M. D., Kilgour, G., Milicich, S. D., and Rae, A. J.: Stratigraphy of the Western Wairakei Geothermal Field: Insights from Recent Drilling in the Greater Te Mihi Area, *Proceedings, New Zealand Geothermal Workshop & New Zealand Geothermal Association Seminar, Auckland, New Zealand* (2007).

Braithwaite, R.L., Wood, C.P., Rosenberg, M.D. and Faure, K.: Porosity and Permeability in the Basement Rocks at the Kawerau and Ohaaki Geothermal Fields, *New Zealand, Proceedings, 24th New Zealand Geothermal Workshop* (2002).

Cole, J.W., and Spinks, K.D.: Caldera Volcanism and Rift Structure in the Taupo Volcanic Zone, New Zealand, *Geological Society, London, Special Publications*, 327(1), (2009), 9-29, doi:10.1144/SP327.2.

Davatzes, N.C., and Hickman, S.: Stress, Fracture, and Fluid-Flow Analysis Using Acoustic and Electrical Image Logs in Hot Fractured Granites of the Coso Geothermal Field, California, U.S.A., *AAPG Memoir*, 92, (2010), 259-293, doi:10.1306/13181288M923134.

Downs, D.T., Rowland, J.V., Wilson, C.J.N., Rosenberg, M.D., Leonard, G.S., and Calvert, A.T.: Evolution of the Intra-Arc Taupo-Reporoa Basin within the Taupo Volcanic Zone of New Zealand, *Geosphere*, 10(1), (2014), 185-206.

Ekstrom, M.P., Dahan, C.A., Chen, M.Y., Lloyd, P.M., and Rossi, D.J.: Formation Imaging with Microelectrical Scanning Arrays, *Log Analyst*, 28, (1987), 294.

Faulds, J.E., Hinz, N.H., Coolbaugh, M.F., Cashman, P.H., Kratt, C., Dering, G., Edwards, J., Mayhew, B., and McLachlan, H.: Assessment of Favorable Structural Settings of Geothermal Systems in the Great Basin, Western USA. *Geothermal Resources Council Transactions*, 35, (2011), 777-783.

Faulkner, D.R., Jackson, C.A.L., Lunn, R.J., Schlische, R.W., Shipton, Z.K., Wibberley, C.A.J., and Withjack, M.O.: A Review of Recent Developments Concerning the Structure, Mechanics and Fluid Flow Properties of Fault Zones, *Journal of Structural Geology*, 32(11), (2010), 1557-1575. doi:10.1016/j.jsg.2010.06.009.

Fossen, H.: Structural Geology, Cambridge University Press, Cambridge, UK (2016), 510 p.

Grindley, G. W.: The Geology, Structure, and Exploitation of the Wairakei Geothermal Field, *New Zealand Geological Survey Bulletin*, 75, (1965), 130 p.

Hernandez, D., Clearwater, J., Burnell, J., Franz, P., Azwar, L., and Marsh, A.: Update on the Modeling of the Rotokawa Geothermal System: 2010–2014, *Proceedings, World Geothermal Congress, Melbourne, Australia* (2015).

Kim, J., Boese, C., Andrews, J., Sepulveda, F., Archer, R. and Malin, P.: Investigation of Fault Structures from Microseismicity in the Wairakei Geothermal Field, New Zealand, Poster, *EGU 2014 General Assembly* (2014).

Kissling, W.M. and Massiot, C.: Permeability Anisotropy and Fluid Dispersion in Pervasively Fractured Lavas, Rotokawa Geothermal Field, New Zealand. *Proceedings, World Geothermal Congress* (2020).

Jolie, E., Klinkmueller, M., Moeck, I., and Bruhn, D.: Linking Gas Fluxes at Earth's Surface With Fracture Zones in an Active Geothermal Field, *Geology*, 44(3), (2016), 187-190. doi:10.1130/G37412.1.

Lamarche, G., Barnes, P.M., and Bull, J.M.: Faulting and Extension Rate over the Last 20,000 Years in the Offshore Whakatane Graben, New Zealand Continental Shelf, *Tectonics*, 25(4), (2006), doi:10.1029/2005TC001886.

Langridge, R.M., Ries, W.F., Litchfield, N.J., Villamor, P., Van Dissen, R.J., Barrell, D., Rattenbury, M.S., Heron, D.W., Haubrock, S., Townsend, D.B., Lee, J.M., Berryman, K.R., Nicol, A., Cox, S.C, and Stirling, M.W.: The New Zealand Active Faults Database, *New Zealand Journal of Geology and Geophysics*, 59(1), (2016), 86-96, doi:10.1080/00288306.2015.1112818.

Lee, J.M., Townsend, D., Bland, K., and Kamp, P.J.J.: Geology of the Hawke's Bay Area, Institute of Geological & Nuclear Sciences 1:250,000 Geological Map, 8, (2011).

Leonard, G.S., Begg, J.G., and Wilson, C.J.J.: Geology of the Rotorua Area. Institute of Geological & Nuclear Sciences 1:250,000 Geological Map, 5, (2010).

Manville, V. and Wilson, C.J.: The 26.5 ka Oruanui Eruption, New Zealand: A Review of the Roles of Volcanism and Climate in the Post-Eruptive Sedimentary Response, *New Zealand Journal of Geology and Geophysics*, 47(3), (2004), 525-547.

Massiot, C., McNamara, D.D., and Lewis, B.: Interpretive Review of the Acoustic Borehole Image Logs Acquired to Date in the Wairakei-Tauhara Geothermal Field, *GNS Science Report*, 2013/04, (2013), 26 p.

Massiot, C., McNamara, D.D., and Lewis, B.: Processing and Analysis of High Temperature Geothermal Acoustic Borehole Image Logs in the Taupo Volcanic Zone, New Zealand, *Geothermics*, 53, (2015), 190-201, doi:10.1016/j.geothermics.2014.05.010.

Massiot, C., McLean, K., McNamara, D.D., Sépulveda, F., and Milicich, S.D.: Discussion Between a Reservoir Engineer and a Geologist: Permeability Identification from Completion Test Data and Borehole Image Logs Integration, *Proceedings, 39th New Zealand Geothermal Workshop, Rotorua, New Zealand* (2017).

Massiot, C., Seebeck, H., Nicol, A., McNamara, D.D., Lawrence, M.J.F., Griffin, A.G., Thrasher, G.P., O'Brien, G., and Viskovic, G.P.D.: Effects of regional and local stress variabilities on fault slip tendency in the southern Taranaki Basin, New Zealand. *Marine and Petroleum Geology*, 107, (2019), 467–483. doi: 10.1016/j.marpetgeo.2019.05.030

McLean, K., and McNamara, D.D.: Fractures Interpreted from Acoustic Formation Imaging Technology: Correlation to Permeability, *Proceedings, Thirty-Sixth Workshop on Geothermal Reservoir Engineering, Auckland, New Zealand* (2011).

McNamara, D.D., Massiot, C., and Lewis, B.: A Structural Review of the Wairakei-Tauhara Geothermal Field, GNS Science Report, 2013/03, (2013), 20 p.

McNamara, D.D., Massiot, C., Lewis, B., and Wallis, I.: Heterogeneity of Structure and Stress in the Rotokawa Geothermal Field, New Zealand. *Journal of Geophysical Research: Solid Earth*, 120(2), (2015), 1243-1262, doi:10.1002/2014JB011480.

McNamara, D.D., Milicich, S.D., Massiot, C., Villamor, P., McLean, K., Sépulveda, F., and Ries, W. F.: Tectonic controls on Taupo Volcanic Zone geothermal expression: Insights from Te Mihi, Wairakei Geothermal Field, *Tectonics*, (2019).

Milicich, S.D., Massiot, C., and McNamara, D.D.: Volcanic texture identification and influence on permeability using a borehole resistivity image log in the Whakamaru Group ignimbrite, Wairakei Geothermal Field, New Zealand. *Proceedings, 43rd Workshop on Geothermal Reservoir Engineering* (2018).

Milicich, S.D., Massiot, C., McNamara, D.D., and Sepulveda, F.: Volcanic Texture Identification and Influence on Permeability Using Borehole Resistivity Image Logs in the Taupo Volcanic Zone, New Zealand. *Proceedings, World Geothermal Congress* (2020)

Milloy, S.F., and Lim, Y.W.: Wairakei-Tauhara Pressure Regime Update, *Proceedings, New Zealand Geothermal Workshop, Auckland, New Zealand* (2012).

Nicol, A., Walsh, J.J., Watterson, J., and Bretan, P.G.: Three-Dimensional Geometry and Growth of Conjugate Normal Faults, *Journal of Structural Geology*, 17(6), (1995), 847-862.

Peacock, D.C.P., and Sanderson, D.J.: Displacements, Segment Linkage and Relay Ramps in Normal Fault Zones, *Journal of Structural Geology*, 13(6), (1991), 721-733.

Risk, G.F.: Electrical resistivity survey of the Wairakei Geothermal Field. *Proceedings of the 6th New Zealand Geothermal Workshop, University of Auckland, New Zealand*, (1984), 123–128.

Risk, G.F.: Electrical resistivity of the Rotokawa Geothermal Field, New Zealand, *Proceedings, 22nd New Zealand Geothermal Workshop, Taupo Volcanic Zone, Rotokawa, New Zealand*, (2000).

Rosenberg, M.D., Bignall, G., and Rae, A.J.: The Geological Framework of the Wairakei–Tauhara Geothermal System, New Zealand. *Geothermics*, 38(1), (2009), 72-84, doi:10.1016/j.geothermics.2009.01.001.

Rosenberg, M.: Volcanic and Tectonic Perspectives on the Age and Evolution of the Wairakei-Tauhara Geothermal System, PhD thesis, Victoria University of Wellington, Wellington, New Zealand (2017).

Rowland, J.V., and Sibson, R.H.: Extensional Fault Kinematics within the Taupo Volcanic Zone, New Zealand: Soft-Linked Segmentation of a Continental Rift System, *New Zealand Journal of Geology and Geophysics*, 44(2), (2001), 271-283. doi:10.1080/00288306.2001.9514938.

Seebeck, H.C., Nicol, A., Villamor, P., Ristau, J., and Pettinga, J.: Structure and Kinematics of the Taupo Rift, New Zealand, *Tectonics*, 33(6), (2014), 1178-1199, doi:10.1002/2014TC003569.

Sepulveda, F., Andrews, J., Kim, J., Siega, C., and Milloy, S. F. (2015). Spatial-temporal Characteristics of Microseismicity (2009-2014) of the Wairakei Geothermal Field, New Zealand. *World Geothermal Congress 2015*, (2015).

Terzaghi, R.D.: Sources of Error in Joint Surveys, *Geotechnique*, 15(3), (1965), 287-304, doi:10.1680/geot.1965.15.3.287.

Townend, J., and Zoback, M.D.: How Faulting Keeps the Crust Strong, *Geology*, 28(5), (2000), 399-402, doi:10.1130/0091-7613(2000)28<399:HFKTCS>2.0.CO;2.

Villamor, P. and Berryman, K.R.: Late Quaternary geometry and kinematics of faults at the southern termination of the Taupo Volcanic Zone, New Zealand, *New Zealand Journal of Geology and Geophysics*, 49 (1), 1-21. (2006).

Villamor, P., Clark, K., Watson, M., Rosenberg, M., Lukovic, B., Ries, W., Gonzalez, A., Milicich, S.D., McNamara, D.D., Pummer, B., and Sepulveda, F.: New Zealand Geothermal Power Plants as Critical Facilities: An Active Fault Avoidance Study in the Wairakei Geothermal Field, New Zealand, *Proceedings, World Geothermal Congress, Melbourne, Australia* (2015).

Villamor, P., Nicol, A., Seebeck, H., Rowland, J., Townsend, D., Massiot, C., McNamara, D.D., Milicich, S.D., Ries, W., and Alcaraz, S.: Tectonic Structure and Permeability in the Taupō Rift: New Insights from Analysis of LIDAR Derived DEMs, *Proceedings, 39th New Zealand Geothermal Workshop, Rotorua, New Zealand* (2017a).

Villamor, P., Berryman, K.R., Ellis, S.M., Schreurs, G., Wallace, L.M., Leonard, G.S., Langridge, R.M., and Ries, W.F.: Rapid Evolution of Subduction-Related Continental Intraarc Rifts: The Taupo Rift, New Zealand, *Tectonics*, 36(10), (2017b), 2250-2272.

Wallace, L. M., Beavan, J., McCaffrey, R., and Darby, D.: Subduction Zone Coupling and Tectonic Block Rotations in the North Island, New Zealand, *Journal of Geophysical Research. Solid Earth*, 109(B12), (2004), B12406, doi:10.1029/2004JB003241.

Williams, C.A., Eberhart-Phillips, D., Bannister, S., Barker, D.H., Henrys, S., Reyners, M. and Sutherland, R.: Revised interface geometry for the Hikurangi subduction zone, New Zealand. *Seismological Research Letters*, 84, (2013), 1066-1073.

Wallis, I.C., McNamara, D., Rowland, J.V., and Massiot, C.: The Nature of Fracture Permeability in the Basement Greywacke at Kawerau Geothermal Field, New Zealand, *Proceedings, 37th Workshop on Geothermal Reservoir Engineering, Stanford, CA (*2012).

Wilson, C.J.N., Rogan, A.M., Smith, I.E.M., Northey, D.J., Nairn, I.A., and Houghton, B.F.: Caldera Volcanoes of the Taupo Volcanic Zone, New Zealand, *Journal of Geophysical Research. Solid Earth and Planets*, 89(B10), (1984), 8463-8484.

Wilson, C.J.N., Houghton, B.F., McWilliams, M.O., Lanphere, M.A., Weaver, S.D., and Briggs, R.M. (1995). Volcanic and structural evolution of Taupo Volcanic Zone, New-Zealand: a review. *Journal of Volcanology and Geothermal Research*, 68(1–3), 1–28. doi: 10.1016/0377-0273(95)00006-g

Wilson, C.J.N., and Rowland, J.V.: The Volcanic, Magmatic and Tectonic Setting of the Taupo Volcanic Zone, New Zealand, Reviewed from a Geothermal Perspective, *Geothermics*, 59(B), (2016), 168-187, doi:10.1016/j.geothermics.2015.06.013.

Zemaneck, J., Glen Jr., E.E., Norton, L.J., and Cardwell, R.L.: Formation Evaluation by Inspection with the Borehole Televiewer, *Geophysics*, 35, (1970), 254-269, doi:10 .1190/1.1440089.